DIGITAL ACCESS TO SCHOLARSHIP AT HARVARD
DASH.HARVARD.EDU

HARVARD LIBRARY
Office for Scholarly Communication

MR Scanner Systems Should Be Adequately Characterized in Diffusion-MRI of the Breast

Citation

Giannelli, Marco, Roberto Sghedoni, Chiara Iacconi, Mauro Iori, Antonio Claudio Traino, Maria Guerrisi, Mario Mascalchi, Nicola Toschi, and Stefano Diciotti. 2014. "MR Scanner Systems Should Be Adequately Characterized in Diffusion-MRI of the Breast." PLoS ONE 9 (1): e86280. doi:10.1371/journal.pone.0086280. http://dx.doi.org/10.1371/journal.pone.0086280.

Published Version

doi:10.1371/journal.pone.0086280

Permanent link

http://nrs.harvard.edu/urn-3:HUL.InstRepos:11879664

Terms of Use

This article was downloaded from Harvard University's DASH repository, and is made available under the terms and conditions applicable to Other Posted Material, as set forth at http://nrs.harvard.edu/urn-3:HUL.InstRepos:dash.current.terms-of-use#LAA

Share Your Story

The Harvard community has made this article openly available.
Please share how this access benefits you. Submit a story .

Accessibility

OPEN ACCESS Freely available online

PLOS ONE

MR Scanner Systems Should Be Adequately Characterized in Diffusion-MRI of the Breast

Marco Giannelli[1]*, Roberto Sghedoni[2], Chiara Iacconi[3], Mauro Iori[2], Antonio Claudio Traino[1], Maria Guerrisi[4], Mario Mascalchi[5], Nicola Toschi[4,6,7], Stefano Diciotti[5,8]

1 Medical Physics Unit, Pisa University Hospital ''Azienda Ospedaliero-Universitaria Pisana'', Pisa, Italy, **2** Department of Oncology and Advanced Techniques, Medical Physics Unit, IRCCS-Arcispedale Santa Maria Nuova, Reggio Emilia, Italy, **3** Division of Radiology, Breast Unit, Massa Hospital, Azienda USL Massa e Carrara, Massa, Italy, **4** Department of Biomedicine and Prevention, Medical Physics Section, University of Rome ''Tor Vergata'', Rome, Italy, **5** Department of Clinical and Experimental Biomedical Sciences, University of Florence, Florence, Italy, **6** Department of Radiology, Athinoula A. Martinos Center for Biomedical Imaging, Boston, Massachusetts, United States of America, **7** Harvard Medical School, Boston, Massachusetts, United States of America, **8** Department of Electrical, Electronic, and Information Engineering ''Guglielmo Marconi'', University of Bologna, Cesena, Italy

Abstract

Breast imaging represents a relatively recent and promising field of application of quantitative diffusion-MRI techniques. In view of the importance of guaranteeing and assessing its reliability in clinical as well as research settings, the aim of this study was to specifically characterize how the main MR scanner system-related factors affect quantitative measurements in diffusion-MRI of the breast. In particular, phantom acquisitions were performed on three 1.5 T MR scanner systems by different manufacturers, all equipped with a dedicated multi-channel breast coil as well as acquisition sequences for diffusion-MRI of the breast. We assessed the accuracy, inter-scan and inter-scanner reproducibility of the mean apparent diffusion coefficient measured along the main orthogonal directions (<ADC>) as well as of diffusion-tensor imaging (DTI)-derived mean diffusivity (MD) measurements. Additionally, we estimated spatial non-uniformity of <ADC> ($NU_{<ADC>}$) and MD (NU_{MD}) maps. We showed that the signal-to-noise ratio as well as overall calibration of high strength diffusion gradients system in typical acquisition sequences for diffusion-MRI of the breast varied across MR scanner systems, introducing systematic bias in the measurements of diffusion indices. While <ADC> and MD values were not appreciably different from each other, they substantially varied across MR scanner systems. The mean of the accuracies of measured <ADC> and MD was in the range [−2.3%,11.9%], and the mean of the coefficients of variation for <ADC> and MD measurements across MR scanner systems was 6.8%. The coefficient of variation for repeated measurements of both <ADC> and MD was < 1%, while $NU_{<ADC>}$ and NU_{MD} values were <4%. Our results highlight that MR scanner system-related factors can substantially affect quantitative diffusion-MRI of the breast. Therefore, a specific quality control program for assessing and monitoring the performance of MR scanner systems for diffusion-MRI of the breast is highly recommended at every site, especially in multicenter and longitudinal studies.

Citation: Giannelli M, Sghedoni R, Iacconi C, Iori M, Traino AC, et al. (2014) MR Scanner Systems Should Be Adequately Characterized in Diffusion-MRI of the Breast. PLoS ONE 9(1): e86280. doi:10.1371/journal.pone.0086280

Editor: Gayle E. Woloschak, Northwestern University Feinberg School of Medicine, United States of America

Received May 23, 2013; **Accepted** December 12, 2013; **Published** January 28, 2014

Copyright: © 2014 Giannelli et al. This is an open-access article distributed under the terms of the Creative Commons Attribution License, which permits unrestricted use, distribution, and reproduction in any medium, provided the original author and source are credited.

Funding: The authors have no support or funding to report.

Competing Interests: The authors have declared that no competing interests exist.

* E-mail: m.giannelli@ao-pisa.toscana.it

Introduction

In magnetic resonance imaging (MRI), ''diffusion'' (i.e. the random, thermally-induced displacements of water molecules over time) [1] represents an extraordinarily sensitive contrast mechanism, and the exquisite structural detail it affords has proven useful in a vast number of clinical as well as research applications, especially in neuroimaging [2]. Currently, diffusion-MRI is a promising and potentially useful MRI technique for improving the diagnostic accuracy of breast imaging without administering contrast agents [3–8]. Indeed, previous studies have shown a potential role of quantitative diffusion-MRI in differentiating between benign and malignant breast lesions [9–12], with the majority of malignant lesions showing reduced diffusion when compared to benign lesions, and diffusion-MRI may aid in identifying patients with low grade ductal carcinoma in situ (DCIS) as compared to high grade DCIS, hence contributing to risk-stratification in DCIS [13,14]. Some studies have revealed an inverse correlation between the cellularity of breast cancer and diffusion indices [15,16], and diffusion indices have been seen to vary significantly according to various histopathological and immunohistochemical tumour features [17]. In locally advanced breast cancer, another potential application of diffusion-MRI is in the evaluation and assessment of the early response of cancer to neoadjuvant chemotherapy [18–20]. Previous studies [21,22] have reported a detectable increase of diffusion which manifested itself before quantifiable decrease in tumour size, and the diffusion change was observed as early as right upon completion of the first cycle of neoadjuvant chemotherapy. Moreover, preliminary studies have suggested that diffusion may be used as a biomarker for pre-treatment prediction of response to neoadjuvant chemotherapy in patients with locally advanced breast cancer [5,23], although this hypothesis needs further validation [24]. Diffusion-MRI has also shown potential for evaluating residual breast cancer following neoadjuvant chemotherapy [25].

Several factors, both in data acquisition and processing, can influence the accuracy and precision of quantitative diffusion-MRI measurements [26–31]. In particular, it should be noted that the signal-to-noise ratio (SNR) as well as the overall degree of calibration of the high strength diffusion gradients system (which are intrinsically linked to all stages of the diffusion-MRI pipeline, from sequence design through data analysis) can directly and systematically bias the measurement of diffusion indices [32]. Accordingly, some studies have emphasized the importance of implementing specific diffusion-MRI related quality control protocols as well as correction methods [33–44], which should be put into practice in addition to standard quality assurance routines in order to guarantee the reliability of quantitative diffusion-MRI measurements. Furthermore, in diffusion-MRI studies, a time- and site-dependency of MR scanner system performance can introduce bias in diffusion-MRI measurements, increase the variance of measured diffusion indices and substantially reduce the power of statistical inference for detecting group differences [30]. In this context, a number of *in vivo* studies have analyzed intra-scanner variability of diffusion-MRI measurements of the brain [27,28,45–53]. Moreover, given that the integration of multicenter data would greatly improve the sensitivity of diffusion-MRI studies, recent clinical investigations have specifically evaluated the inter-scanner reproducibility of measurements of different diffusion-tensor imaging (DTI)-derived indices in the human brain [54–60]. In diffusion-MRI of the body, some *in vivo* studies have evaluated the inter-scan reproducibility of measurements of diffusion indices of the abdomen [61–64], liver [65–67], prostate [68], anal canal [69] and kidney [70]. However, so far, only a few clinical studies [71–74] have specifically investigated the reliability of diffusion-MRI measurements in the breast in terms of inter-scan reproducibility as well as intra- and inter-observer reproducibility.

In view of the fact that breast imaging represents a relatively recent field of application of quantitative diffusion-MRI techniques, and based on the importance of guaranteeing and assessing its reliability in clinical as well as research investigations, the aim of this study was to specifically characterize how the main MR scanner system-related factors affect quantitative measurements in diffusion-MRI of the breast. In particular, we evaluated the accuracy, inter-scan and inter-scanner reproducibility of measurements of phantom diffusion indices performed on 1.5 T MR scanner systems by different manufacturers, all equipped with a dedicated multi-channel breast coil as well as acquisition sequences for diffusion-MRI of the breast.

Materials and Methods

2.1. MR scanner systems and phantom

All diffusion-MRI acquisitions were performed on three commercial 1.5 T MR scanner systems by three different manufacturers, operating in three distinct centers: scanner-A [GE Signa HDx TwinSpeed (GE Medical Systems - Milwaukee, WI, USA) with 50 mT/m maximum gradient strength and 150 T/m/s slew rate], scanner-B [Philips Achieva (Philips Medical Systems - Eindhoven, the Nederlands) with 66 mT/m maximum gradient strength and 90 T/m/s slew rate] and scanner-C [Siemens Avanto (Siemens Healthcare - Erlangen, Germany) with 45 mT/m maximum gradient strength and 200 T/m/s slew rate]. All MR scanner systems were equipped with a dedicated multi-channel breast coil with 8, 7 and 4 elements for scanner-A, scanner-B and scanner-C, respectively. For each MR scanner system, standard maintenance and quality assurance procedures were routinely performed.

The same doped (per 1000 g H_2O distilled: 1.25 g $NiSO_4 \times 6H_2O$ + 5 g NaCl) isotropic water phantom (i.e. two identical cylindrical bottles with diameter 11.5 cm and length 20 cm) was employed in all acquisitions.

2.2. Data acquisition

Images from different MR scanner systems were obtained using pulse sequences provided by the manufacturers. For diffusion-weighted image acquisition, we used a 2D axial spin echo - echo planar imaging sequence, sensitized to diffusion (DWI-SE-EPI) through strong magnetic field gradient pulses. The acquisition protocols and parameters are reported in Table 1.

For each MR scanner system, all acquisitions were performed on the same day in order to avoid any mid- and long-term changes in scanner performance as well as any potential variability induced by phantom repositioning. The phantom (i.e. two cylindrical bottles as described above) was stored in the scanner room for at least 24 hours prior to scanning and was positioned in the gantry 1 hour before acquisition. The centre of each of the two cylindrical bottles was placed in the centre of each of the two sides of the breast coil and secured using foam padding. The central slice of the acquisition slab (21 slices) was placed at the centre of the two bottles (Figure 1). The temperature of the scanner bore was recorded during data acquisition.

2.2.1. SNR and calibration of diffusion gradients system. In order to evaluate SNR as well as the calibration of the high strength diffusion gradients system in each MR scanner, the axial DWI-SE-EPI sequence (Table 1) was acquired both without (*b-value* = 0 s/mm^2) and with (*b-value* = 850 s/mm^2) sensitization to diffusion along each of the main orthogonal directions (readout/left-right, phase-encoding/anterior-posterior, slice-selection/head-foot). In order to improve SNR, we employed a number of excitations (NEX) equal to 14. The above acquisitions were repeated obtaining a total of 5 measurements.

2.2.2. Accuracy, inter-scan and inter-scanner reproducibility of diffusion-MRI measurements. In order to assess the accuracy, inter-scan and inter-scanner reproducibility of measurements of conventional mean apparent diffusion

Table 1. Axial 2D diffusion-weighted spin echo - echo planar imaging (DWI-SE-EPI) sequence: acquisition parameters for scanner-A, scanner-B and scanner-C.

	Scanner-A	Scanner-B	Scanner-C
TR (ms)	8000	8000	8000
TE (ms)	81	81	83
BW (Hz/pixel)	3906	2905	2170
b-value (s/mm^2)	850	850	850
FOV (mm×mm)	350×350	350×350	350×350
Matrix	128×128	128×128	128×128
Slice thickness (mm)	5	5	5
Interslice gap (mm)	0	0	0
Number of slices	21	21	21
K space sampling	5/8	5/8	5/8
Parallel imaging	ASSET	SENSE	mSENSE
Acceleration factor	2	2	2
Phase encoding direction	anterior/posterior	anterior/posterior	anterior/posterior

doi:10.1371/journal.pone.0086280.t001

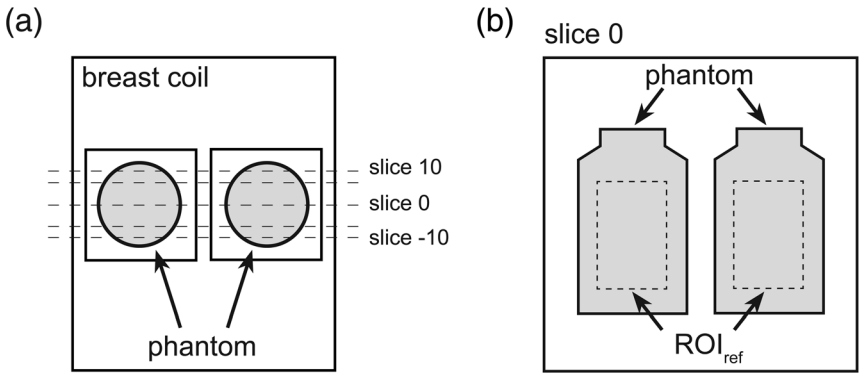

Figure 1. Schematic description of a) breast coil, phantom and acquisition slab (21 slices), as well as b) ROI_{ref} positioning.
doi:10.1371/journal.pone.0086280.g001

coefficient (ADC) measured along the main orthogonal directions (<ADC>) as well as DTI-derived indices (which a few breast studies have preliminarily incorporated in their scanning protocols [72,73,75–77]) additional diffusion-weighted images along each of the main orthogonal directions and DTI data sets were acquired using the DWI-SE-EPI sequence (Table 1) with *b-value* = 850 s/mm^2. For each MR scanner system, DTI acquisitions of the DWI-SE-EPI sequence with sensitization to diffusion along 6 non-collinear and non-coplanar directions [72,75,76] were performed. For <ADC> as well as DTI measurements, an additional acquisition of the DWI-SE-EPI sequence without sensitization to diffusion (*b-value* = 0 s/mm^2) was carried out. In order to guarantee a constant acquisition time, the NEX value was 7 and 4 for <ADC> and DTI data sets, respectively. The entire set of acquisitions was repeated obtaining a total of 5 measurements for both <ADC> and DTI data.

2.3. Image processing and analysis

Except for diffusion tensor estimation, all processing and analysis of diffusion-MRI data was performed using custom scripts developed in MATLAB 7.1 (MathWorks, Natick, MA, USA).

In order to better evaluate inter-scanner variability of diffusion-MRI measurements independently of temperature (T_a) during data acquisition, ADC measured along each of the main orthogonal directions, <ADC> and DTI-derived mean diffusivity (MD) values were normalized to a reference value corresponding to a temperature of 22°C (at which the phantom diffusion coefficient, D_0, is equal to $2.14\pm0.03\times10^{-3}$ mm^2/s) [78]. In particular, for each MR scanner system, we used an analytical equation derived by fitting experimental water diffusion coefficients measured at different temperature values with the Arrhenius activation law to obtain the true phantom diffusion coefficient at T_a (D_a) [78]. Given that for an isotropic phantom the ratio (R) between the value of a diffusion index measured at T_a and D_a depends exclusively on the ratios ($R_b^{i=1\text{-}n}$, n = 1, 3 and 6 for ADC measured along each of the main orthogonal directions, <ADC> and MD, respectively) between the nominal and the effective *b-value* applied along the diffusion sensitized directions (which can reasonably be considered independent of temperature), the normalized values of diffusion indices were calculated as RD_0.

All analyses were carried out in the central slice of the acquired phantom volume, within a reference region of interest (ROI_{ref}) that consisted of two rectangles (size 29×41 voxels), each placed in the centre of the image of the bottle on each of two sides of the breast coil (Figure 1).

2.3.1. SNR and maps of ADC along each of the main orthogonal directions. The SNR was calculated using non-diffusion-weighted (b_0) images. Conventional approaches to evaluate SNR are based on the signal statistics in one or two separate large regions of interest of a single image or the signal statistics in a large region of interest of a difference image of two repeated acquisitions [79,80]. In order to take into account spatial variations in SNR (which can be substantial in acquisitions performed using multi-channel coils and parallel imaging techniques) [81], maps of SNR in small adjacent ROIs of 8×8 voxels (SNR_{ROI}) were computed as previously described [81,82]:

$$SNR_{ROI} = \frac{mean_{\mathbf{r}\in ROI}[mean_{k=1-5}(S_{b_0}(\mathbf{r},k))]}{mean_{\mathbf{r}\in ROI}[std\,dev_{k=1-5}(S_{b_0}(\mathbf{r},k)]} \qquad (1)$$

where $S_{b0}(\mathbf{r},k)$ is the signal of the voxel at position $\mathbf{r}$ within the selected ROI for the *k*th repetition of the b_0 image. The overall SNR was computed as the mean value of SNR_{ROI} within ROI_{ref}.

For each repetition ($k = 1$–5), ADC maps along each of the main orthogonal directions [$ADC_{i,k}(\mathbf{r})$ - $i = 1$, readout/left-right; $i = 2$, phase-encoding/anterior-posterior; $i = 3$, slice-selection/head-foot] were computed. For the *i*th direction, the mean, $(ADC_i)_{mean}$, and standard deviation, $(ADC_i)_{SD}$, images across repetitions were calculated. Then, the overall ADC along the *i*th diffusion weighting direction (ADC_i) was obtained as the average $(ADC_i)_{mean}$ within ROI_{ref}. Furthermore, the overall percent coefficient of variation for repeated measurements of ADC along the *i*th diffusion weighting direction was computed as follows:

$$CV_{ADC_i} = mean_{\mathbf{r}\in ROI_{ref}}\left[\frac{(ADC_i)_{SD}(\mathbf{r})}{(ADC_i)_{mean}(\mathbf{r})}\right]\times 100 \quad (\%) \qquad (2)$$

The spatial non-uniformity levels of maps of ADC along each of the main orthogonal directions were evaluated by adapting a method proposed by Magnusson and Olsson [83]. The $ADC_{i,k}$ maps were smoothed using a low-pass spatial filter with a 3×3 kernel which reduces noise by computing the mean value of a voxel and its 8 neighbours, and replacing the value of the voxel with this mean. Then, the mean value (C) within ROI_{ref} was estimated. For each voxel, the deviation from this value was calculated as the absolute value of [100×(voxel value - C)/C], obtaining a new image which represents the absolute value of the percentage deviation from C. The mean value of this new image within ROI_{ref} was recorded, obtaining the non-uniformity value of $ADC_{i,k}$ maps ($NU_{ADC_{i,k}}$) for each diffusion weighting direction

($i = 1$–3) and repetition ($k = 1$–5). Finally, for each diffusion weighting direction, the overall non-uniformity degree (NU_{ADC_i}) was estimated as the mean of $NU_{ADC_{i,k}}$ across repetitions.

2.3.2. Maps of <ADC>, MD and FA. For each repetition ($k = 1$–5), the mean ADC along the main orthogonal directions [$<ADC>_k(\mathbf{r})$] was calculated voxel-wise. The overall mean ADC (<ADC>) and its coefficient of variation for repeated measurements ($CV_{<ADC>}$) were calculated as described above for ADC_i and CV_{ADC_i}, respectively. Moreover, the overall spatial non-uniformity degree of <ADC> maps ($NU_{<ADC>}$) was estimated using the same method employed for calculating NU_{ADC_i}.

In order to estimate the diffusion tensor, we adopted a method similar to that described in previous breast DTI studies [72,76]. In particular, we performed the standard steps implemented in the diffusion toolbox (FDT) of FSL 4.1.4 (Oxford Centre for Functional Magnetic Resonance Imaging of the Brain (FMRIB) software library) [84,85] using the weighted linear least square approach. For each repetition ($k = 1$–5), the mean diffusivity [$MD_k(\mathbf{r})$] and fractional anisotropy [$FA_k(\mathbf{r})$] were computed voxel-wise. Then, the overall mean diffusivity (MD) and fractional anisotropy (FA) were calculated as described for ADC_i. The coefficient of variation for repeated measurements of MD (CV_{MD}) and spatial non-uniformity of MD maps (NU_{MD}) were then obtained using the same procedure adopted for CV_{ADC_i} and NU_{ADC_i} calculation.

2.3.3. Statistical analysis. Any significant difference in quality control data and measured diffusion metrics, both across the main orthogonal directions within a single MR scanner system and across MR scanner systems, was assessed through a one-way analysis of variance (ANOVA). When the ANOVA revealed a significant difference ($p<0.05$), a post-hoc analysis was performed using the two sample t-test, with Bonferroni correction for multiple comparisons. For each MR scanner system, any significant difference between <ADC> and MD maps was assessed similarly. The one-sample t-test, with Bonferroni correction for multiple comparisons, was used to evaluate any significant difference between the true diffusion indices and estimated diffusion indices.

Results

3.1. SNR and calibration of diffusion gradients system

The SNR (mean value ± standard deviation within ROI_{ref}) was 242±55, 184±26 and 309±60 for scanner-A, scanner-B and scanner-C, respectively. The SNR values varied significantly across MR scanner systems (ANOVA: $p<0.0001$ – post-hoc analysis: $p<0.001$ for scanner-A vs scanner-B, scanner-A vs scanner-C and scanner-B vs scanner-C).

For each of the main orthogonal directions ($i = 1$–3), the ADC_i, CV_{ADC_i} and NU_{ADC_i} results are reported in Figure 2, Figure 3 and Figure 4, respectively. ADC_i ($i = 1$–3) values varied significantly with diffusion gradient direction for scanner-A (ANOVA: $p<0.0001$ – post-hoc analysis: $p<0.001$ for $i = 1$ vs $i = 2$, $i = 1$ vs $i = 3$, $i = 2$ vs $i = 3$), scanner-B (ANOVA: $p<0.0001$ – post-hoc analysis: $p<0.001$ for $i = 1$ vs $i = 2$, $i = 1$ vs $i = 3$, $i = 2$ vs $i = 3$) and scanner-C (ANOVA: $p<0.0001$ – post-hoc analysis: $p<0.01$ and $p<0.001$ for $i = 1$ vs $i = 2$ and $i = 1$ vs $i = 3$, $i = 2$ vs $i = 3$, respectively). Moreover, except for ADC_1 for scanner-C ($p>0.05$), all measured ADC_i values were significantly ($p<0.05$) different from the known phantom diffusion coefficient. For each MR scanner system, CV_{ADC_i} and NU_{ADC_i} values varied significantly with diffusion gradient direction (ANOVA: $p<0.0001$ – post-hoc analysis: $p<0.001$ for $i = 1$ vs $i = 2$, $i = 1$ vs $i = 3$, $i = 2$ vs $i = 3$).

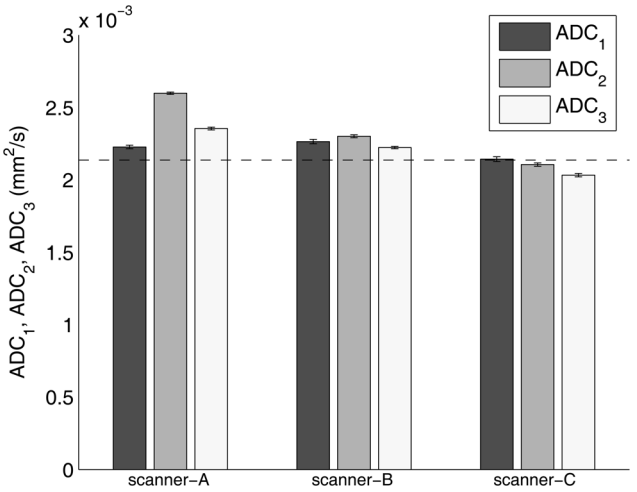

Figure 2. Phantom ADC along each of the main orthogonal directions (ADC_i - $i = 1$, readout/left-right; $i = 2$, phase-encoding/anterior-posterior; $i = 3$, slice-selection/head-foot) for scanner-A, scanner-B and scanner-C. The bar charts depict the mean of the average value within ROI_{ref} ± standard deviation across five repetitions. The dashed line represents the known phantom diffusion coefficient ($2.14 \pm 0.03 \times 10^{-3}$ mm^2/s) at the reference temperature value of 22°C.
doi:10.1371/journal.pone.0086280.g002

3.2. Accuracy, inter-scan and inter-scanner reproducibility of diffusion-MRI measurements

Both <ADC> and MD data are reported in Figure 5. Within each MR scanner system, <ADC> and MD values were not significantly different ($p>0.05$) from each other. On the other hand, <ADC> and MD values varied significantly across MR scanner systems (ANOVA: $p<0.0001$ – post-hoc analysis: $p<0.001$ for scanner-A vs scanner-B, scanner-A vs scanner-C and scanner-B vs scanner-C). Both <ADC> and MD values were significantly ($p<0.01$) different from their true value, with an

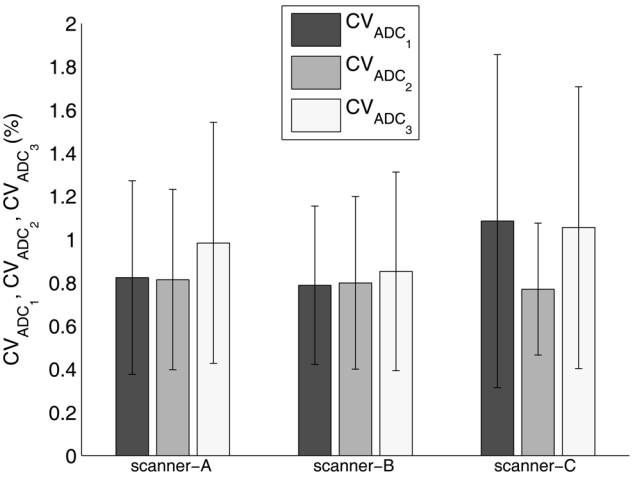

Figure 3. Coefficient of variation for repeated measurements of phantom ADC along each of the main orthogonal directions (CV_{ADC_i} - $i = 1$, readout/left-right; $i = 2$, phase-encoding/anterior-posterior; $i = 3$, slice-selection/head-foot) for scanner-A, scanner-B and scanner-C. The bar charts depict the mean value ± standard deviation within ROI_{ref}.
doi:10.1371/journal.pone.0086280.g003

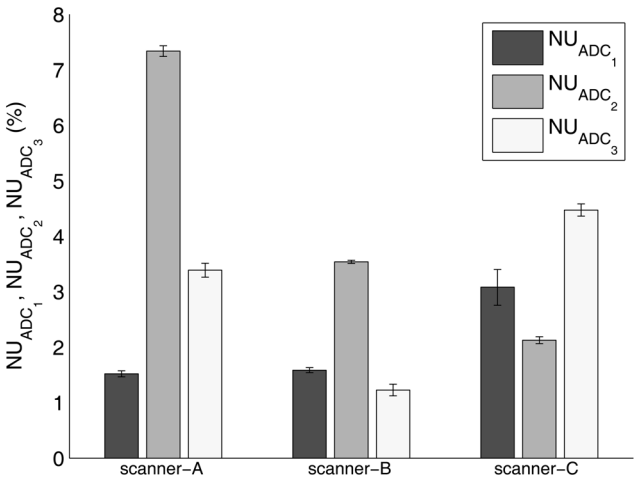

Figure 4. Non-uniformity of maps of phantom ADC along each of the main orthogonal directions (NU_{ADC_i} - *i* = 1, readout/left-right; *i* = 2, phase-encoding/anterior-posterior; *i* = 3, slice-selection/head-foot) for scanner-A, scanner-B and scanner-C. The bar charts depict the mean value ± standard deviation across five repetitions.
doi:10.1371/journal.pone.0086280.g004

accuracy (percentage difference between the measured and known diffusion value) ranging from -2.6% to 12.0%.

The $CV_{<ADC>}$ and CV_{MD} results as well as $NU_{<ADC>}$ and NU_{MD} results are reported in Table 2. For each MR scanner system, $CV_{<ADC>}$ and CV_{MD} differed significantly ($p<0.001$) with values which were less than 1%. Moreover, $CV_{<ADC>}$ and CV_{MD} varied significantly across MR scanner systems (ANOVA: $p<0.0001$ – post-hoc analysis: $p<0.001$ for scanner-A vs scanner-B, scanner-A vs scanner-C and scanner-B vs scanner-C). For scanner-A and scanner-B, $NU_{<ADC>}$ and NU_{MD} were not significantly ($p>0.05$) different, whereas, for scanner-C, $NU_{<ADC>}$ was significantly ($p<0.01$) lower than NU_{MD}. Furthermore, both $NU_{<ADC>}$ (ANOVA: $p<0.0001$ – post-hoc analysis: $p<0.001$ and $p>0.05$ for scanner-A vs scanner-B, scanner-A vs scanner-C and scanner-B vs scanner-C, respectively) and NU_{MD} (ANOVA: $p<0.0001$ – post-hoc analysis: $p<0.001$ for scanner-A vs scanner-B, scanner-A vs scanner-C and scanner-B vs scanner-C) varied significantly across MR scanner systems, with values which were less than 4%.

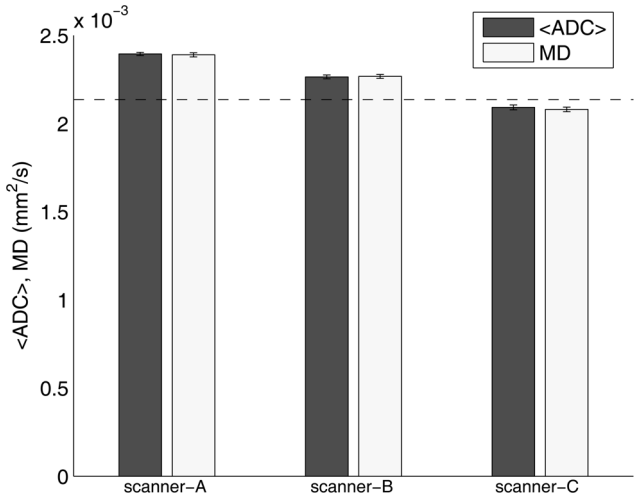

Figure 5. Mean ADC along the main orthogonal directions (<ADC>) as well as mean diffusivity (MD) of the phantom for scanner-A, scanner-B and scanner-C. The bar charts depict the mean of the average value within ROI_{ref} ± standard deviation across five repetitions. The dashed line represents the known phantom diffusion coefficient ($2.14\pm0.03\times10^{-3}$ mm^2/s) at the reference temperature value of 22°C.
doi:10.1371/journal.pone.0086280.g005

For each MR scanner system, the overall FA of the phantom was significantly ($p<0.001$) greater than 0. Moreover, FA values varied significantly across MR scanner systems (ANOVA: $p<0.0001$ – post-hoc analysis: $p<0.001$ for scanner-A vs scanner-B, scanner-A vs scanner-C and scanner-B vs scanner-C). In particular, FA values (mean of the average value within ROI_{ref} ± standard deviation across five repetitions) were 0.086 ± 0.001, 0.050 ± 0.001 and 0.076 ± 0.001 for scanner-A, scanner-B and scanner-C, respectively.

Discussion

A number of *in vivo* studies have evaluated the reliability of diffusion-MRI measurements in the brain as well as body [27,28,45–70,86]. However, a more specific and careful evaluation of the reliability of diffusion-MRI measurements of the breast would be of practical interest. Recently, O'Flynn *et al.* [71] have assessed the mid-term reproducibility and inter-observer variability of ADC measurements of fibroglandular tissue at 3 T, obtaining a within-subject coefficient of variation of 22–25% and a kappa value (κ) of 0.83. Partridge *et al.* [72] have evaluated the reproducibility of DTI-derived parameter measurements in normal breast tissue at 1.5 T after repositioning and rescanning, reporting a between-scan coefficient of variation of 4.5% and 11.4% for MD and FA, respectively. Tagliafico *et al.* [73] have reported a between-scan coefficient of variation of 15% and 30% for MD and FA measurements in normal breast tissue at 3 T, respectively; moreover, when looking at intra-/inter-observer variability, the κ values were 0.82–0.89/0.73–0.83 and 0.60–0.84/0.64–0.80 for MD and FA, respectively. Additionally, when measuring ADC at 1.5 T in breast carcinomas, Petralia *et al.* [74] estimated an intra- and inter-observer variability of 1.1% and 2%, respectively. It should be noted that assessing and guaranteeing reliability of quantitative diffusion-MRI measurements, which is a prerequisite for successful clinical as well as research studies, necessarily includes a characterization of the MR scanner system. Indeed, although *in vivo* studies can evaluate repeatability and reproducibility of diffusion-MRI measurements in a clinical setting (which are fundamental elements toward carrying out longitudinal as well as multicenter studies), such studies do not allow to address measurement accuracy as well as some of the main characteristics

Table 2. $CV_{<ADC>}$ and CV_{MD} results [mean value (standard deviation within ROI_{ref})] as well as $NU_{<ADC>}$ and NU_{MD} results [mean value (standard deviation across five repetitions)] for scanner-A, scanner-B and scanner-C.

	Scanner-A	Scanner-B	Scanner-C
$CV_{<ADC>}$ (%)	0.69 (0.34)	0.64 (0.31)	0.81 (0.38)
CV_{MD} (%)	0.53 (0.28)	0.67 (0.32)	0.92 (0.58)
$NU_{<ADC>}$ (%)	3.70 (0.04)	1.70 (0.08)	1.83 (0.14)
NU_{MD} (%)	3.65 (0.09)	1.67 (0.08)	2.52 (0.09)

doi:10.1371/journal.pone.0086280.t002

of MR scanner system (e.g. the SNR or the calibration of high strength diffusion gradients system) that can systematically bias quantitative diffusion-MRI measurements [30,32]. A limited number of studies have reported phantom data specific to the characterization of MR scanner systems for diffusion-MRI of the brain as well as the body [34–41,43,57,58,87,88]. However, in diffusion-MRI of the breast, only a few clinical studies have incorporated a basic verification of the calibration of diffusion gradients [11,22,72,89,90].

To the best of our knowledge, this is the first phantom study which carries out multiple and specific quality controls in order to characterize in detail different 1.5 T MR scanner systems by three different manufacturers, all equipped with a dedicated multi-channel breast coil as well as acquisition sequence for quantitative diffusion-MRI of the breast. In particular, for each MR scanner system, we evaluated the calibration of high strength diffusion gradients for the three main orthogonal axes along which diffusion-sensitizing gradients can be applied. Then, we assessed how the MR scanner system-related factors affect the accuracy, inter-scan and inter-scanner reproducibility of diffusion measurements of <ADC> as well as of DTI measurements of MD. We used acquisition protocols and parameters typically employed in diffusion-MRI of the breast, which, except for small differences in readout bandwidth (BW) values, were similar for all MR scanner systems. As suggested by Bogner *et al.* [89], we employed a *b-value* of 850 s/mm^2. For all acquisitions, we used the same homogeneous and isotropic phantom with known diffusion coefficient, allowing a proper evaluation of the accuracy of estimated diffusion indices as well as non-uniformity of maps of diffusion indices. The diffusion coefficient of the phantom at room temperature ($\sim 2\times10^{-3}$ mm^2/s) is similar to water diffusion coefficient in normal breast tissue ($1.8–2.1\times10^{-3}$ mm^2/s), while it is slightly higher than water diffusion coefficient in malign as well benign breast tissue ($0.9–1.7\times10^{-3}$ mm^2/s) [7,22,72,89,91]. In this context, as previously described by Delakis *et al.* [35], the use of a phantom with a relatively high diffusion coefficient is recommended in order to improve the sensitivity to any discrepancies in measured diffusion indices induced by differences between the nominal and the effective *b-value* applied along the diffusion sensitized directions.

Diffusion-MRI measurements are affected by an inherently low SNR. In particular, both precision and accuracy of diffusion indices can depend on SNR [27–29,82,92–94]. Therefore, we began by characterizing each MR scanner system in terms of SNR. In particular, the overall SNR of scanner-B was 24% and 40% lower than that of scanner-A and scanner-C, respectively. Interestingly, based on the BW values of the acquisition protocols (Table 1), scanner-A (highest BW value) was expected to show the lowest SNR across MR scanner systems. Therefore, SNR results cannot be ascribed to differences in BW values only, and are likely to also reflect different overall sensitivities of the breast coils.

All MR scanner systems showed a high short term stability of the performance of diffusion gradients. For each MR scanner system, the overall coefficient of variation for repeated measurements of ADC along each of the main orthogonal directions was less than 1.1% (Figure 3). Nonetheless, for each MR scanner system and direction (readout/left-right, phase-encoding/anterior-posterior, slice-selection/head-foot) except for ADC measurements along the readout/left-right direction for scanner-C, we revealed a significant difference between the measured ADC and the true diffusion coefficient. Moreover, for each MR scanner system, the entity of this difference varied significantly with diffusion direction (Figure 2). This effect, when quantified in terms of the coefficient of variation of ADC measurements across the main orthogonal directions, was more relevant for scanner-A (7.9%) as compared to scanner-B (1.7%) and scanner-C (2.7%). As a whole, these results indicate a mismatch between the theoretically assumed and the effective *b-value*. This could originate from errors in diffusion gradients amplitude, eddy current fields, concomitant field terms and cross terms between diffusion gradients and imaging gradients [2,32,87,88,95]. These factors are direction-dependent and can have deleterious effects that are more prominent at the high gradient strengths usually employed in diffusion-MRI [2,32]. In addition, any diffusion gradient non-uniformity is expected to yield a spatial variation in measured diffusion indices. For each MR scanner system, we observed that the spatial non-uniformity values of maps of ADC along each of the main orthogonal directions depended significantly on the diffusion weighting direction. Scanner-A showed a relatively high spatial non-uniformity value (7.3%) of ADC along the phase-encoding/anterior-posterior direction, while for both scanner-B and scanner-C the degree of non-uniformity of ADC along each diffusion weighting direction was less than 4.5% (Figure 4). In general, when DWI-SE-EPI sequences (Table 1) are acquired, the high strength diffusion gradients system belonging to each MR scanner system presented an overall mis-calibration (not documented by standard maintenance procedures and quality assurance routines), which can affect diffusion indices measurement. Therefore, in order to improve the reliability of quantitative diffusion-MRI of the breast, suitable correction methods could be employed [34,36,37,40].

For each MR scanner system, the coefficient of variation for short term repeated measurements of both <ADC> and MD was less than 1% (Table 2), while previous clinical studies [71–73] which measured breast diffusion indices have reported a between-scan coefficient of variation in the range 5–15%. The greater experimental variability of *in vivo* diffusion-MRI measurements when compared to our phantom study is likely due to patient repositioning, manual ROI positioning and motion induced effects.

For every MR scanner system, the spatial non-uniformities of <ADC> and MD maps were less than 4% (Table 2). For scanner-A and scanner-B, non-uniformities of <ADC> and MD maps were not significantly different. Conversely, for scanner-C, the non-uniformity of the <ADC> map (1.8%) was significantly lower than the non-uniformity of the MD map (2.5%). For each MR scanner system, we did not reveal any significant difference between estimated <ADC> and MD values, with an absolute percentage difference between <ADC> and MD of less than 0.6%. This indicates a correct pulse timing when using multiple oblique diffusion gradients as employed in DTI, and may suggest the negligibility of cross-term effects between diffusion and imaging gradients along different directions [26,95,96]. However, the accuracy of <ADC> and MD measurements varied significantly with the MR scanner system (Figure 5). In particular, the mean value of <ADC> and MD accuracies was 11.9%, 6.0% and -2.3% for scanner-A, scanner-B and scanner-C, respectively, while the mean value of the coefficients of variation for <ADC> and MD measurements across MR scanner systems was 6.8%. Previous phantom studies of diffusion-MRI both using a head coil [35,36,38–40,43,58,87] and a body coil [34,43] have reported accuracy values of estimated diffusion indices ranging from −15% to 30%. Other *in vivo* studies of the brain [45,46,54–59] have reported a coefficient of variation in MD and FA across different MR scanner systems in the ranges 4–15% and 5–29%, respectively. In this context, it is important to note that the differences in diffusion indices reported in previous clinical diffusion-MRI studies of the breast range from 5% to 45% [9–13,17,21–23,25,76]. Therefore, a comparison of breast diffusion-MRI data

from different centers should be performed with great caution. Moreover, during the planning of a multicenter study, the accuracy of diffusion-MRI measurements should be carefully assessed in every participating center. Additionally, in longitudinal studies, a periodic monitoring of the accuracy of measured diffusion indices is highly recommended. In a meta-analysis of 13 studies dealing with quantitative diffusion-MRI in the differential diagnosis of breast lesions, Chen *et al.* [91] have shown that a) the ADC values of benign lesions ranged from 1×10^{-3} mm^2/s to 1.82×10^{-3} mm^2/s, b) the cutoff values for differentiating malignant from benign lesions ranged from 0.9×10^{-3} mm^2/s to 1.76×10^{-3} mm^2/s, and that c) the sensitivity and specificity ranged from 63% to 100% and 46% to 97%, respectively. This heterogeneity could be due to differences in patient characteristics and diagnostic criteria, as well as to different diffusion-MRI acquisition and analysis methods. However, we hypothesize that potential differences in MR scanner system-related factors between different MR scanner systems, which can systematically bias accuracy and precision of diffusion-MRI measurements, may contribute to explaining the results heterogeneity reported by Chen *et al.* [91].

Besides DTI-based measurements of MD, we also performed diffusion anisotropy estimation, and the overall FA value of the isotropic phantom (true FA = 0) was found to be significantly greater than 0 for every MR scanner system. This could reflect effects of relatively low SNR (high SNR has been shown to reduce the brain anisotropy overestimation due to noise at a *b-value* typically used in clinical DTI examinations, $\sim$1000 s/mm^2) [93,94], as well as errors in diffusion gradients amplitude (which can result in mimicking anisotropy). While for each MR scanner system FA values were less than 0.09, they were significantly different among MR scanner systems. In particular, data acquired on scanner-B resulted in the lowest FA estimate ($\sim$0.05).

Conclusions

Although breast imaging is an appealing and promising application field of diffusion-MRI, only few *in vivo* studies have recently evaluated the inter-scan reproducibility as well as intra- and inter-observer reproducibility of diffusion measurements of the breast [71–74]. In this phantom study, we characterized in detail three 1.5 T MR scanner systems by three different manufacturers, all equipped with a dedicated multi-channel breast coil as well as acquisition sequences for quantitative diffusion-MRI of the breast. The SNR as well as overall calibration of high strength diffusion gradients system varied substantially across MR scanner systems, introducing systematic bias in measurements of diffusion indices. We note that *in vivo* diffusion-MRI measurements of the breast can also depend on other non-MR scanner system-related factors – such as subject-related artifacts (e.g. motion and cardiac pulsation, physiological noise), perfusion and non-Gaussian processes – that could further increase the variability in diffusion measurements. Nonetheless, in order to improve the reliability of quantitative breast diffusion-MRI and, hence, the sensitivity of clinical studies, a specific and periodic quality control program for characterizing and monitoring the performance of breast coil and high strength diffusion gradients of MR scanner system is highly recommended at every site, especially before multicenter studies are tackled as well as during longitudinal studies. In this context, we agree with Jones [30] and De Santis *et al.* [41] who have recently emphasized that the quality control culture in diffusion-MRI remains limited. Therefore, we feel that in diffusion-MRI, which is a truly quantitative technique, enabling a suitable and dedicated quality assurance program at every site would represent a major step toward the effective use of every MR scanner system as a "measurement tool", hence further improving and strengthening the capabilities of this powerful diagnostic modality.

Supporting Information

Figure S1 Maps of phantom ADC along each of the main orthogonal directions ($i=1$, readout/left-right; $i=2$, phase-encoding/anterior-posterior; $i=3$, slice-selection/head-foot), calculated using the first ($k=1$) of 5 repetitions ($ADC_{i,1}$), for scanner-A (left pane), scanner-B (middle pane) and scanner-C (right pane). In order to facilitate visual assessment, the figure depicts a zoomed region (located on one side of the breast coil) of the phantom containing one of the two rectangular ROIs (highlighted in red) which make up ROI_{ref}.
(TIF)

Acknowledgments

The authors would like to thank Dr. Gianni Borasi for the professional suggestion and stimulus to undertake this study. Also, the authors are grateful to Dr. Piero Ghedin and anonymous reviewers for expert technical assistance and constructive/helpful comments, respectively.

Author Contributions

Conceived and designed the experiments: M. Giannelli RS SD. Performed the experiments: M. Giannelli RS. Analyzed the data: M. Giannelli SD. Contributed reagents/materials/analysis tools: M. Giannelli RS CI MI ACT M. Guerrisi MM NT SD. Wrote the paper: M. Giannelli NT SD. Performed image processing: SD. Performed critical revision and final approval of the manuscript: M. Giannelli RS CI MI ACT M. Guerrisi MM NT SD.

References

1. Einstein A, Fürth R (1956) Investigations on the theory of Brownian movement. New York, N.Y.: Dover Publications.
2. Johansen-Berg H, Behrens TEJ (2009) Diffusion MRI: From quantitative measurement to in-vivo neuroanatomy: Elsevier Science.
3. Partridge SC, DeMartini WB, Kurland BF, Eby PR, White SW, et al. (2009) Quantitative diffusion-weighted imaging as an adjunct to conventional breast MRI for improved positive predictive value. AJR Am J Roentgenol 193: 1716–1722.
4. Ei Khouli RH, Jacobs MA, Mezban SD, Huang P, Kamel IR, et al. (2010) Diffusion-weighted imaging improves the diagnostic accuracy of conventional 3.0-T breast MR imaging. Radiology 256: 64–73.
5. Iacconi C, Giannelli M, Marini C, Cilotti A, Moretti M, et al. (2010) The role of mean diffusivity (MD) as a predictive index of the response to chemotherapy in locally advanced breast cancer: a preliminary study. Eur Radiol 20: 303–308.
6. Pereira FP, Martins G, Carvalhaes de Oliveira Rde V (2011) Diffusion magnetic resonance imaging of the breast. Magn Reson Imaging Clin N Am 19: 95–110.
7. Woodhams R, Ramadan S, Stanwell P, Sakamoto S, Hata H, et al. (2011) Diffusion-weighted imaging of the breast: principles and clinical applications. Radiographics 31: 1059–1084.
8. Kazama T, Kuroki Y, Kikuchi M, Sato Y, Nagashima T, et al. (2012) Diffusion-weighted MRI as an adjunct to mammography in women under 50 years of age: an initial study. J Magn Reson Imaging 36: 139–144.
9. Woodhams R, Matsunaga K, Iwabuchi K, Kan S, Hata H, et al. (2005) Diffusion-weighted imaging of malignant breast tumors: the usefulness of apparent diffusion coefficient (ADC) value and ADC map for the detection of malignant breast tumors and evaluation of cancer extension. J Comput Assist Tomogr 29: 644–649.
10. Rubesova E, Grell AS, De Maertelaer V, Metens T, Chao SL, et al. (2006) Quantitative diffusion imaging in breast cancer: a clinical prospective study. J Magn Reson Imaging 24: 319–324.
11. Marini C, Iacconi C, Giannelli M, Cilotti A, Moretti M, et al. (2007) Quantitative diffusion-weighted MR imaging in the differential diagnosis of breast lesion. Eur Radiol 17: 2646–2655.

12. Partridge SC, Demartini WB, Kurland BF, Eby PR, White SW, et al. (2010) Differential diagnosis of mammographically and clinically occult breast lesions on diffusion-weighted MRI. J Magn Reson Imaging 31: 562–570.
13. Iima M, Le Bihan D, Okumura R, Okada T, Fujimoto K, et al. (2011) Apparent diffusion coefficient as an MR imaging biomarker of low-risk ductal carcinoma in situ: a pilot study. Radiology 260: 364–372.
14. Rahbar H, Partridge SC, Demartini WB, Gutierrez RL, Allison KH, et al. (2012) In vivo assessment of ductal carcinoma in situ grade: a model incorporating dynamic contrast-enhanced and diffusion-weighted breast MR imaging parameters. Radiology 263: 374–382.
15. Guo Y, Cai Y-Q, Cai Z-L, Gao Y-G, An N-Y, et al. (2002) Differentiation of clinically benign and malignant breast lesions using diffusion-weighted imaging. J Magn Reson Imaging 16: 172–178.
16. Woodhams R, Kakita S, Hata H, Iwabuchi K, Umeoka S, et al. (2009) Diffusion-weighted imaging of mucinous carcinoma of the breast: evaluation of apparent diffusion coefficient and signal intensity in correlation with histologic findings. AJR Am J Roentgenol 193: 260–266.
17. Martincich L, Deantoni V, Bertotto I, Redana S, Kubatzki F, et al. (2012) Correlations between diffusion-weighted imaging and breast cancer biomarkers. Eur Radiol 22: 1519–1528.
18. Chenevert TL, Meyer CR, Moffat BA, Rehemtulla A, Mukherji SK, et al. (2002) Diffusion MRI: a new strategy for assessment of cancer therapeutic efficacy. Mol Imaging 1: 336–343.
19. Theilmann RJ, Borders R, Trouard TP, Xia G, Outwater E, et al. (2004) Changes in water mobility measured by diffusion MRI predict response of metastatic breast cancer to chemotherapy. Neoplasia 6: 831–837.
20. Manton DJ, Chaturvedi A, Hubbard A, Lind MJ, Lowry M, et al. (2006) Neoadjuvant chemotherapy in breast cancer: early response prediction with quantitative MR imaging and spectroscopy. Br J Cancer 94: 427–435.
21. Pickles MD, Gibbs P, Lowry M, Turnbull LW (2006) Diffusion changes precede size reduction in neoadjuvant treatment of breast cancer. Magn Reson Imaging 24: 843–847.
22. Sharma U, Danishad KK, Seenu V, Jagannathan NR (2009) Longitudinal study of the assessment by MRI and diffusion-weighted imaging of tumor response in patients with locally advanced breast cancer undergoing neoadjuvant chemotherapy. NMR Biomed 22: 104–113.
23. Park SH, Moon WK, Cho N, Song IC, Chang JM, et al. (2010) Diffusion-weighted MR imaging: pretreatment prediction of response to neoadjuvant chemotherapy in patients with breast cancer. Radiology 257: 56–63.
24. Iacconi C, Giannelli M (2011) Can diffusion-weighted MR imaging be used as a biomarker for predicting response to neoadjuvant chemotherapy in patients with locally advanced breast cancer? Radiology 259: 303–304.
25. Woodhams R, Kakita S, Hata H, Iwabuchi K, Kuranami M, et al. (2010) Identification of residual breast carcinoma following neoadjuvant chemotherapy: diffusion-weighted imaging–comparison with contrast-enhanced MR imaging and pathologic findings. Radiology 254: 357–366.
26. Le Bihan D, Poupon C, Amadon A, Lethimonnier F (2006) Artifacts and pitfalls in diffusion MRI. J Magn Reson Imaging 24: 478–488.
27. Farrell JAD, Landman BA, Jones CK, Smith SA, Prince JL, et al. (2007) Effects of signal-to-noise ratio on the accuracy and reproducibility of diffusion tensor imaging-derived fractional anisotropy, mean diffusivity, and principal eigenvector measurements at 1.5 T. J Magn Reson Imaging 26: 756–767.
28. Landman BA, Farrell JAD, Jones CK, Smith SA, Prince JL, et al. (2007) Effects of diffusion weighting schemes on the reproducibility of DTI-derived fractional anisotropy, mean diffusivity, and principal eigenvector measurements at 1.5T. Neuroimage 36: 1123–1138.
29. Landman BA, Farrell JAD, Huang H, Prince JL, Mori S (2008) Diffusion tensor imaging at low SNR: nonmonotonic behaviors of tensor contrasts. Magn Reson Imaging 26: 790–800.
30. Jones DK (2010) Precision and accuracy in diffusion tensor magnetic resonance imaging. Top Magn Reson Imaging 21: 87–99.
31. Jones DK, Cercignani M (2010) Twenty-five pitfalls in the analysis of diffusion MRI data. NMR Biomed 23: 803–820.
32. Jones DK (2010) Diffusion MRI : Theory, Methods, and Applications: Theory, Methods, and Applications: Oxford University Press, USA.
33. Schmithorst VJ, Dardzinski BJ (2002) Automatic gradient preemphasis adjustment: a 15-minute journey to improved diffusion-weighted echo-planar imaging. Magn Reson Med 47: 208–212.
34. Bammer R, Markl M, Barnett A, Acar B, Alley MT, et al. (2003) Analysis and generalized correction of the effect of spatial gradient field distortions in diffusion-weighted imaging. Magn Reson Med 50: 560–569.
35. Delakis I, Moore EM, Leach MO, De Wilde JP (2004) Developing a quality control protocol for diffusion imaging on a clinical MRI system. Phys Med Biol 49: 1409–1422.
36. Nagy Z, Weiskopf N, Alexander DC, Deichmann R (2007) A method for improving the performance of gradient systems for diffusion-weighted MRI. Magn Reson Med 58: 763–768.
37. Wu YC, Alexander AL (2007) A method for calibrating diffusion gradients in diffusion tensor imaging. J Comput Assist Tomogr 31: 984–993.
38. Chenevert TL, Galban CJ, Ivancevic MK, Rohrer SE, Londy FJ, et al. (2011) Diffusion coefficient measurement using a temperature-controlled fluid for quality control in multicenter studies. J Magn Reson Imaging 34: 983–987.
39. Wang ZJ, Seo Y, Chia JM, Rollins NK (2011) A quality assurance protocol for diffusion tensor imaging using the head phantom from American College of Radiology. Med Phys 38: 4415–4421.
40. Mohammadi S, Nagy Z, Moller HE, Symms MR, Carmichael DW, et al. (2012) The effect of local perturbation fields on human DTI: characterisation, measurement and correction. Neuroimage 60: 562–570.
41. De Santis S, Evans CJ, Jones DK (2012) RAPID: A routine assurance pipeline for imaging of diffusion. Magn Reson Med.
42. Walker L, Curry M, Nayak A, Lange N, Pierpaoli C, et al. (2012) A framework for the analysis of phantom data in multicenter diffusion tensor imaging studies. Hum Brain Mapp.
43. Malyarenko D, Galban CJ, Londy FJ, Meyer CR, Johnson TD, et al. (2013) Multi-system repeatability and reproducibility of apparent diffusion coefficient measurement using an ice-water phantom. J Magn Reson Imaging 37: 1238–1246.
44. Lauzon CB, Asman AJ, Esparza ML, Burns SS, Fan Q, et al. (2013) Simultaneous analysis and quality assurance for diffusion tensor imaging. PLoS One 8: e61737.
45. Pfefferbaum A, Adalsteinsson E, Sullivan EV (2003) Replicability of diffusion tensor imaging measurements of fractional anisotropy and trace in brain. J Magn Reson Imaging 18: 427–433.
46. Cercignani M, Bammer R, Sormani MP, Fazekas F, Filippi M (2003) Inter-sequence and inter-imaging unit variability of diffusion tensor MR imaging histogram-derived metrics of the brain in healthy volunteers. AJNR Am J Neuroradiol 24: 638–643.
47. Marenco S, Rawlings R, Rohde GK, Barnett AS, Honea RA, et al. (2006) Regional distribution of measurement error in diffusion tensor imaging. Psychiatry Res 147: 69–78.
48. Bonekamp D, Nagae LM, Degaonkar M, Matson M, Abdalla WM, et al. (2007) Diffusion tensor imaging in children and adolescents: reproducibility, hemispheric, and age-related differences. Neuroimage 34: 733–742.
49. Bisdas S, Bohning DE, Besenski N, Nicholas JS, Rumboldt Z (2008) Reproducibility, interrater agreement, and age-related changes of fractional anisotropy measures at 3T in healthy subjects: effect of the applied b-value. AJNR Am J Neuroradiol 29: 1128–1133.
50. Ciccarelli O, Parker GJ, Toosy AT, Wheeler-Kingshott CA, Barker GJ, et al. (2003) From diffusion tractography to quantitative white matter tract measures: a reproducibility study. Neuroimage 18: 348–359.
51. Heiervang E, Behrens TEJ, Mackay CE, Robson MD, Johansen-Berg H (2006) Between session reproducibility and between subject variability of diffusion MR and tractography measures. Neuroimage 33: 867–877.
52. Vaessen MJ, Hofman PA, Tijssen HN, Aldenkamp AP, Jansen JF, et al. (2010) The effect and reproducibility of different clinical DTI gradient sets on small world brain connectivity measures. Neuroimage 51: 1106–1116.
53. Landman BA, Huang AJ, Gifford A, Vikram DS, Lim IA, et al. (2011) Multi-parametric neuroimaging reproducibility: a 3-T resource study. Neuroimage 54: 2854–2866.
54. Sasaki M, Yamada K, Watanabe Y, Matsui M, Ida M, et al. (2008) Variability in absolute apparent diffusion coefficient values across different platforms may be substantial: a multivendor, multi-institutional comparison study. Radiology 249: 624–630.
55. Pagani E, Hirsch JG, Pouwels PJ, Horsfield MA, Perego E, et al. (2010) Intercenter differences in diffusion tensor MRI acquisition. J Magn Reson Imaging 31: 1458–1468.
56. Vollmar C, O'Muircheartaigh J, Barker GJ, Symms MR, Thompson P, et al. (2010) Identical, but not the same: Intra-site and inter-site reproducibility of fractional anisotropy measures on two 3.0 T scanners. NeuroImage 51: 1384–1394.
57. Teipel SJ, Reuter S, Stieltjes B, Acosta-Cabronero J, Ernemann U, et al. (2011) Multicenter stability of diffusion tensor imaging measures: a European clinical and physical phantom study. Psychiatry Res 194: 363–371.
58. Zhu T, Hu R, Qiu X, Taylor M, Tso Y, et al. (2011) Quantification of accuracy and precision of multi-center DTI measurements: a diffusion phantom and human brain study. Neuroimage 56: 1398–1411.
59. Fox RJ, Sakaie K, Lee JC, Debbins JP, Liu Y, et al. (2012) A validation study of multicenter diffusion tensor imaging: reliability of fractional anisotropy and diffusivity values. AJNR Am J Neuroradiol 33: 695–700.
60. Huang L, Wang X, Baliki MN, Wang L, Apkarian AV, et al. (2012) Reproducibility of structural, resting-state BOLD and DTI data between identical scanners. PLoS One 7: e47684.
61. Braithwaite AC, Dale BM, Boll DT, Merkle EM (2009) Short- and midterm reproducibility of apparent diffusion coefficient measurements at 3.0-T diffusion-weighted imaging of the abdomen. Radiology 250: 459–465.
62. Bilgili MY (2012) Reproductibility of apparent diffusion coefficients measurements in diffusion-weighted MRI of the abdomen with different b values. Eur J Radiol 81: 2066–2068.
63. Rosenkrantz AB, Oei M, Babb JS, Niver BE, Taouli B (2011) Diffusion-weighted imaging of the abdomen at 3.0 Tesla: image quality and apparent diffusion coefficient reproducibility compared with 1.5 Tesla. J Magn Reson Imaging 33: 128–135.
64. Miquel ME, Scott AD, Macdougall ND, Boubertakh R, Bharwani N, et al. (2012) In vitro and in vivo repeatability of abdominal diffusion-weighted MRI. Br J Radiol 85: 1507–1512.

65. Kwee TC, Takahara T, Koh DM, Nievelstein RA, Luijten PR (2008) Comparison and reproducibility of ADC measurements in breathhold, respiratory triggered, and free-breathing diffusion-weighted MR imaging of the liver. J Magn Reson Imaging 28: 1141–1148.
66. Kim SY, Lee SS, Byun JH, Park SH, Kim JK, et al. (2010) Malignant hepatic tumors: short-term reproducibility of apparent diffusion coefficients with breath-hold and respiratory-triggered diffusion-weighted MR imaging. Radiology 255: 815–823.
67. Kim SY, Lee SS, Park B, Kim N, Kim JK, et al. (2012) Reproducibility of measurement of apparent diffusion coefficients of malignant hepatic tumors: effect of DWI techniques and calculation methods. J Magn Reson Imaging 36: 1131–1138.
68. Gibbs P, Pickles MD, Turnbull LW (2007) Repeatability of echo-planar-based diffusion measurements of the human prostate at 3 T. Magn Reson Imaging 25: 1423–1429.
69. Goh V, Tam E, Taylor NJ, Stirling JJ, Simcock IC, et al. (2012) Diffusion tensor imaging of the anal canal at 3 tesla: feasibility and reproducibility of anisotropy measures. J Magn Reson Imaging 35: 820–826.
70. Cutajar M, Clayden JD, Clark CA, Gordon I (2011) Test-retest reliability and repeatability of renal diffusion tensor MRI in healthy subjects. Eur J Radiol 80: e263–268.
71. O'Flynn EA, Morgan VA, Giles SL, deSouza NM (2012) Diffusion weighted imaging of the normal breast: reproducibility of apparent diffusion coefficient measurements and variation with menstrual cycle and menopausal status. Eur Radiol 22: 1512–1518.
72. Partridge SC, Murthy RS, Ziadloo A, White SW, Allison KH, et al. (2010) Diffusion tensor magnetic resonance imaging of the normal breast. Magn Reson Imaging 28: 320–328.
73. Tagliafico A, Rescinito G, Monetti F, Villa A, Chiesa F, et al. (2012) Diffusion tensor magnetic resonance imaging of the normal breast: reproducibility of DTI-derived fractional anisotropy and apparent diffusion coefficient at 3.0 T. Radiol Med 117: 992–991003.
74. Petralia G, Bonello L, Summers P, Preda L, Malasevschi A, et al. (2011) Intraobserver and interobserver variability in the calculation of apparent diffusion coefficient (ADC) from diffusion-weighted magnetic resonance imaging (DW-MRI) of breast tumours. Radiol Med 116: 466–476.
75. Baltzer PA, Schafer A, Dietzel M, Grassel D, Gajda M, et al. (2011) Diffusion tensor magnetic resonance imaging of the breast: a pilot study. Eur Radiol 21: 1–10.
76. Partridge SC, Ziadloo A, Murthy R, White SW, Peacock S, et al. (2010) Diffusion tensor MRI: preliminary anisotropy measures and mapping of breast tumors. J Magn Reson Imaging 31: 339–347.
77. Eyal E, Shapiro-Feinberg M, Furman-Haran E, Grobgeld D, Golan T, et al. (2012) Parametric diffusion tensor imaging of the breast. Invest Radiol 47: 284–291.
78. Tofts PS, Lloyd D, Clark CA, Barker GJ, Parker GJ, et al. (2000) Test liquids for quantitative MRI measurements of self-diffusion coefficient in vivo. Magn Reson Med 43: 368–374.
79. Price RR, Axel L, Morgan T, Newman R, Perman W, et al. (1990) Quality assurance methods and phantoms for magnetic resonance imaging: report of AAPM nuclear magnetic resonance Task Group No. 1. Med Phys 17: 287–295.
80. Och JG, Clarke GD, Sobol WT, Rosen CW, Mun SK (1992) Acceptance testing of magnetic resonance imaging systems: report of AAPM Nuclear Magnetic Resonance Task Group No. 6. Med Phys 19: 217–229.
81. Dietrich O, Raya JG, Reeder SB, Reiser MF, Schoenberg SO (2007) Measurement of signal-to-noise ratios in MR images: influence of multichannel coils, parallel imaging, and reconstruction filters. J Magn Reson Imaging 26: 375–385.
82. Giannelli M, Belmonte G, Toschi N, Pesaresi I, Ghedin P, et al. (2011) Technical note: DTI measurements of fractional anisotropy and mean diffusivity at 1.5 T: comparison of two radiofrequency head coils with different functional designs and sensitivities. Med Phys 38: 3205–3211.
83. Magnusson P, Olsson LE (2000) Image analysis methods for assessing levels of image plane nonuniformity and stochastic noise in a magnetic resonance image of a homogeneous phantom. Med Phys 27: 1980–1994.
84. Behrens TE, Woolrich MW, Jenkinson M, Johansen-Berg H, Nunes RG, et al. (2003) Characterization and propagation of uncertainty in diffusion-weighted MR imaging. Magn Reson Med 50: 1077–1088.
85. Smith SM, Jenkinson M, Woolrich MW, Beckmann CF, Behrens TEJ, et al. (2004) Advances in functional and structural MR image analysis and implementation as FSL. Neuroimage 23 Suppl 1: 208–219.
86. Takao H, Hayashi N, Kabasawa H, Ohtomo K (2012) Effect of scanner in longitudinal diffusion tensor imaging studies. Hum Brain Mapp 33: 466–477.
87. Baron CA, Lebel RM, Wilman AH, Beaulieu C (2012) The effect of concomitant gradient fields on diffusion tensor imaging. Magn Reson Med 68: 1190–1201.
88. Meier C, Zwanger M, Feiweier T, Porter D (2008) Concomitant field terms for asymmetric gradient coils: consequences for diffusion, flow, and echo-planar imaging. Magn Reson Med 60: 128–134.
89. Bogner W, Gruber S, Pinker K, Grabner G, Stadlbauer A, et al. (2009) Diffusion-weighted MR for differentiation of breast lesions at 3.0 T: how does selection of diffusion protocols affect diagnosis? Radiology 253: 341–351.
90. Sinha S, Lucas-Quesada FA, Sinha U, DeBruhl N, Bassett LW (2002) In vivo diffusion-weighted MRI of the breast: potential for lesion characterization. J Magn Reson Imaging 15: 693–704.
91. Chen X, Li WL, Zhang YL, Wu Q, Guo YM, et al. (2010) Meta-analysis of quantitative diffusion-weighted MR imaging in the differential diagnosis of breast lesions. BMC Cancer 10: 693.
92. Alexander AL, Lee JE, Wu Y-C, Field AS (2006) Comparison of diffusion tensor imaging measurements at 3.0 T versus 1.5 T with and without parallel imaging. Neuroimaging Clin N Am 16: 299–309.
93. Jones DK, Basser PJ (2004) "Squashing peanuts and smashing pumpkins": how noise distorts diffusion-weighted MR data. Magn Reson Med 52: 979–993.
94. Pierpaoli C, Basser PJ (1996) Toward a quantitative assessment of diffusion anisotropy. Magn Reson Med 36: 893–906.
95. Mattiello J, Basser PJ, Le Bihan D (1997) The b matrix in diffusion tensor echo-planar imaging. Magn Reson Med 37: 292–300.
96. Le Bihan D (1995) Diffusion and perfusion magnetic resonance imaging: applications to functional MRI: Raven Press.